LETTERS

An inhibitor of Bcl-2 family proteins induces regression of solid tumours

Tilman Oltersdorf[1]*, Steven W. Elmore[2]*, Alexander R. Shoemaker[2]*, Robert C. Armstrong[1], David J. Augeri[2], Barbara A. Belli[1], Milan Bruncko[2], Thomas L. Deckwerth[1], Jurgen Dinges[2], Philip J. Hajduk[2], Mary K. Joseph[2], Shinichi Kitada[3], Stanley J. Korsmeyer[4,5], Aaron R. Kunzer[2], Anthony Letai[5], Chi Li[6], Michael J. Mitten[2], David G. Nettesheim[2], ShiChung Ng[2], Paul M. Nimmer[2], Jacqueline M. O'Connor[2], Anatol Oleksijew[2], Andrew M. Petros[2], John C. Reed[3], Wang Shen[2], Stephen K. Tahir[2], Craig B. Thompson[6], Kevin J. Tomaselli[1], Baole Wang[2], Michael D. Wendt[2], Haichao Zhang[2], Stephen W. Fesik[2] & Saul H. Rosenberg[2]

Proteins in the Bcl-2 family are central regulators of programmed cell death[1], and members that inhibit apoptosis, such as Bcl-X_L and Bcl-2, are overexpressed in many cancers and contribute to tumour initiation, progression and resistance to therapy[2]. Bcl-X_L expression correlates with chemo-resistance of tumour cell lines[3], and reductions in Bcl-2 increase sensitivity to anticancer drugs[4] and enhance *in vivo* survival[5]. The development of inhibitors of these proteins as potential anti-cancer therapeutics has been previously explored[6–15], but obtaining potent small-molecule inhibitors has proved difficult owing to the necessity of targeting a protein–protein interaction. Here, using nuclear magnetic resonance (NMR)-based screening, parallel synthesis and structure-based design, we have discovered ABT-737, a small-molecule inhibitor of the anti-apoptotic proteins Bcl-2, Bcl-X_L and Bcl-w, with an affinity two to three orders of magnitude more potent than previously reported compounds[7–15]. Mechanistic studies reveal that ABT-737 does not directly initiate the apoptotic process, but enhances the effects of death signals, displaying synergistic cytotoxicity with chemotherapeutics and radiation. ABT-737 exhibits single-agent-mechanism-based killing of cells from lymphoma and small-cell lung carcinoma lines, as well as primary patient-derived cells, and in animal models, ABT-737 improves survival, causes regression of established tumours, and produces cures in a high percentage of the mice.

Anti-apoptotic family members (for example, Bcl-2 and Bcl-X_L) and a subgroup of pro-apoptotic proteins (for example, Bax and Bak) are α-helical proteins with extensive sequence and structural similarity[16]. A separate pro-apoptotic group has similarity restricted to a single α-helix called the BH3 region (for example, Bad and Bid). These BH3-only proteins initiate apoptosis either by activating pro-apoptotic Bcl-2 proteins or by inhibiting the anti-apoptotic family members[17,18]. Their activity is mediated through the association of the BH3 α-helix of one protein with a large hydrophobic pocket on binding partners[19].

A high-throughput NMR-based method for lead compound discovery called 'SAR by NMR'[20] was used to screen a chemical library to identify small molecules that bind to the hydrophobic BH3-binding groove of Bcl-X_L. 4′-Fluoro-biphenyl-4-carboxylic acid (dissociation constant $K_d = 0.30 \pm 0.03$ mM; mean ± s.d., $n = 3$) and 5,6,7,8-tetrahydro-naphthalen-1-ol ($K_d = 4.3 \pm 1.6$ mM) bind to distinct but proximal subsites within this cleft. The carboxyl group of the 4-biphenylcarboxylic acid binds near Arg 139 of Bcl-X_L, while the 4′-fluorophenyl group occupies a hydrophobic pocket (site 1) formed by Tyr 101, Leu 108, Val 126 and Phe 146 (Fig. 1a). Interestingly, these are the same sites that are occupied by Asp 83 and Leu 78 of a peptide derived from the BH3 region of Bak, two of the three residues most critical for affinity to Bcl-X_L (ref. 19). Similarly, the naphthalene derivative occupies the same hydrophobic region (site 2) as the third critical residue of the Bak peptide, Ile 85.

The SAR by NMR technology is based on the linkage of proximal fragments to achieve high-affinity binding. Substitution of an acylsulphonamide for the biphenyl carboxyl group maintained the correct positioning of the acidic proton while providing an optimal trajectory to site 2 that avoids steric interference by Phe 97. Site-directed parallel synthesis led to the discovery that a 3-nitro-4-(2-phenylthioethyl)aminophenyl group spans the binding sites and efficiently occupies site 2 through hydrophobic collapse and subsequent π–π stacking (Fig. 1b, compound 1).

Compound 1 binds with high affinity to Bcl-X_L (inhibitory constant $K_i = 36 \pm 1.6$ nM; mean ± s.e.m., $n = 3$), but affinity was attenuated by a factor of >280 in the presence of 1% human serum owing to tight binding to domain III of human serum albumin (HSA). To reduce binding to HSA, a structure-based approach was used[21]. The NMR structure of the thioethylamino-2,4-dimethylphenyl analogue of compound 1 complexed with domain III of HSA (Fig. 1c) was compared to the structure of compound 1 bound to Bcl-X_L. The structures revealed portions of the molecule that were solvent-exposed in the Bcl-X_L complex, but surrounded by lipophilic residues in the complex with HSA. These positions (arrows in Fig. 1c) were modified with polar substituents to reduce binding to HSA without affecting affinity for Bcl-X_L. Specifically, a basic 2-dimethylaminoethyl group was appended to the 1-position of the thioethylamino linkage group and the fluorophenyl occupying site 1 was replaced with a substituted piperazine. In addition, to improve the binding to Bcl-2, a lipophilic group was added to the piperazine to access a deep, well-defined pocket identified in three-dimensional structures of Bcl-2/inhibitor complexes (see Supplementary Fig. 2).

The resultant compound, ABT-737 (Fig. 1d), binds with high affinity ($K_i \leq 1$ nM) to Bcl-X_L, Bcl-2 and Bcl-w, but not to the less-homologous proteins Bcl-B, Mcl-1 and A1 ($K_i = 0.46 \pm 0.11$ μM,

[1]Idun Pharmaceuticals, 9380 Judicial Drive, San Diego, California 92121, USA. [2]Global Pharmaceutical Research & Development, Abbott Laboratories, Abbott Park, Illinois 60064, USA. [3]The Burnham Institute, 10901 North Torrey Pines Road, La Jolla, California 92037, USA. [4]Howard Hughes Medical Institute, Harvard Medical School, Boston, Massachusetts 02115, USA. [5]Harvard Medical School, Dana-Farber Cancer Institute, Boston, Massachusetts 02115, USA. [6]Abramson Family Cancer Research Institute, University of Pennsylvania, Philadelphia, Pennsylvania 19104, USA.
*These authors contributed equally to this work.

>1 μM and >1 μM, respectively). Nanomolar activity was retained in the presence of 10% human serum (median inhibitory concentration $IC_{50} = 35 \pm 1$ nM and 103 ± 2 nM for Bcl-X_L and Bcl-2, respectively). The enantiomer (the stereoisomer bearing the opposite configuration of the dimethylaminoethyl group) was less potent ($IC_{50} = 1{,}400 \pm 150$ and 650 ± 70 nM for Bcl-X_L and Bcl-2, respectively, 10% human serum) and was employed as a loss-of-function control in the biological assays described below.

'Activating' BH3 proteins (for example, Bid, Bim) initiate apoptosis by inducing Bax and Bak oligomerization and subsequent cytochrome *c* release, while 'sensitizing' BH3 proteins (for example, Bad and Bik) exert their pro-death function by binding anti-apoptotic Bcl-2 family members, thereby preventing them from sequestering activating BH3 proteins[22]. Thus Bid protein induced cytochrome *c* release from purified mitochondria, which was inhibited by Bcl-2, while a Bad-derived BH3 peptide did not cause cytochrome *c* release by itself (Fig. 2a). However, the Bad BH3 peptide blocked the inhibition of Bid-mediated cytochrome *c* release by Bcl-2. ABT-737 showed the same effect as a Bad-derived BH3 peptide in purified mitochondria. Like the Bad BH3 peptide (but in contrast to a stabilized peptide derived from Bid[14]), ABT-737 antagonized Bcl-2 protection at concentrations ≥10 nM, but did not induce cytochrome *c* release at concentrations up to 1 μM. The enantiomer was significantly less active. ABT-737 also reversed the protection afforded by Bcl-X_L, activity that was completely dependent on Bax or Bak (see Supplementary Fig. 3)[23]. Moreover, the presence of either of these pro-apoptotic proteins proved sufficient to mediate the effects of ABT-737. Thus, like Bad, ABT-737 binds to and inhibits anti-apoptotic Bcl-2 family proteins, but does not directly activate the pro-apoptotic proteins Bax and Bak.

A mammalian two-hybrid system[24] demonstrated that ABT-737 disrupted an intracellular Bcl-2 family protein–protein interaction. ABT-737 inhibited the interaction of GAL 4–Bcl-X_L and VP16–Bcl-X_S by 44 ± 1% and 55 ± 2% at concentrations of 0.1 μM and 1.0 μM, respectively, while the enantiomer exhibited little activity (5 ± 1% inhibition at 3 μM). The mechanism was further validated by confocal time-lapsed microscopy experiments, in which ABT-737 (but not the enantiomer) displaced a GFP-tagged BH3-only protein (Bcl-G_S) from Bcl-X_L localized at mitochondrial surfaces in intact tumour cells (Fig. 2b–g).

ABT-737 and related compounds display synergism with chemotherapeutics and radiation, such that the median effective concentration (EC_{50}) value for cytotoxicity of the chemotherapeutic/radiation is reduced in the presence of ABT-737 (etoposide, 2–13-fold; doxorubicin, 2–4-fold; cisplatin, 2–3-fold, paclitaxel 2–20-fold; radiation, 2–4-fold) in a variety of tumour cell lines (not shown).

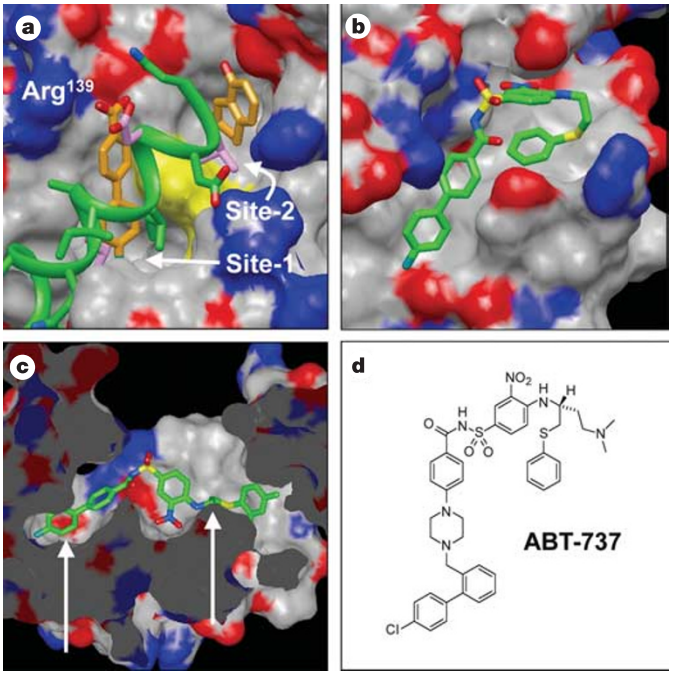

Figure 1 | Generation of ABT-737. a, Connolly surface of the complex of Bcl-X_L with a Bak-derived peptide (GQVGRQLAIIGDDINR, green) overlaid on the ternary complex of Bcl-X_L and NMR-based screening leads (orange). Phe 97 is shown in yellow. Residues of the Bak peptide (Asp 83, Leu 78, Ile 85) critical for binding are shown in magenta. **b**, Connolly surface of the NMR structure of Bcl-X_L complexed with compound 1. **c**, Cutaway Connolly surface for the NMR structure of domain III of HSA bound to the thioethylamino-2,4-dimethylphenyl analogue of compound 1. Arrows indicate proposed sites of modification. **d**, Chemical structure of ABT-737.

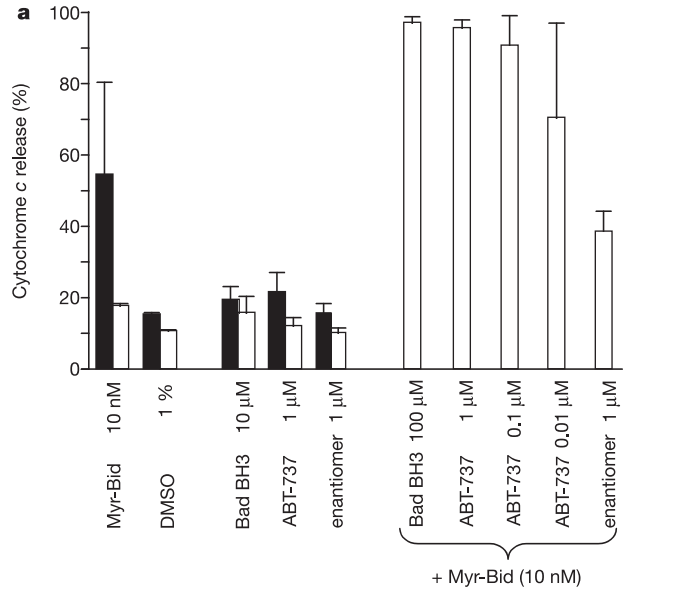

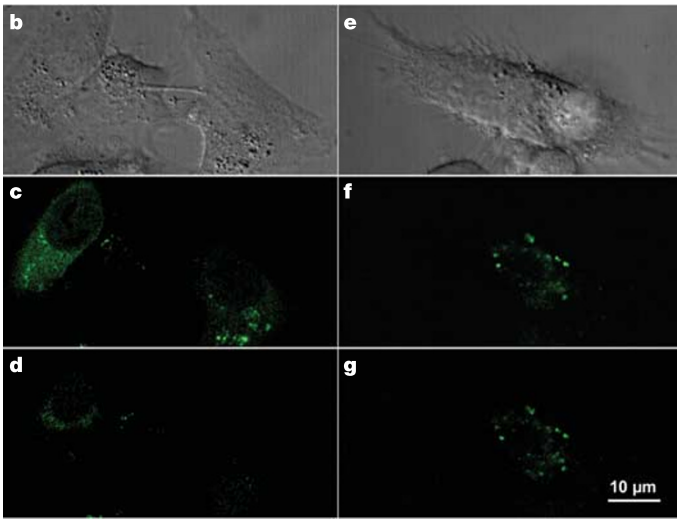

Figure 2 | ABT-737 antagonizes anti-apoptotic Bcl-2 family proteins. **a**, ABT-737 and Bad BH3 peptide do not induce cytochrome *c* release from wild-type (filled bar) or Bcl-2 transfected (open bar) mitochondria, but antagonize the ability of Bcl-2 to inhibit Bid-mediated cytochrome *c* release. Data are mean ± s.d. **b**–**g**, Confocal microscopic images of HeLa cells transfected with Bcl-X_L and GFP-Bcl-G_S visualized with GFP fluorescence. **b**, **e**, Phase-contrast images of untreated cells **c**, **f**, Bcl-G_S fused to GFP displays a punctate pattern coincident with mitochondria. **d**, **g**, ABT-737 (100 nM, **d**) but not the enantiomer (100 nM, **g**) displaces GFP-labelled Bcl-G_S from mitochondria.

This synergism suggests that Bcl-2 family inhibitors may be useful as a component of several chemotherapy regimens. For example, ABT-737 enhanced the cytotoxicity of paclitaxel against A549 NSCLC (non small-cell lung carcinoma) cells by a factor of 4 (Fig. 3a), although ABT-737 alone did not affect cell survival at concentrations up to 1 μM. Because single-agent anti-tumour activity is a more readily achieved clinical endpoint than chemosensitization, we determined whether any tumour cells would be sensitive to our Bcl-2 family inhibitors as single agents. Thus we evaluated the effects of ABT-737 against a diverse panel of human tumour cell lines. In contrast to the weak activity observed with many solid tumour lines such as A549 cells, ABT-737 displayed potent single-agent activity against the subset of cell lines representing lymphoid malignancies and SCLC.

Defective apoptosis is frequently associated with malignancies originating from B-lymphocytes. Follicular lymphoma, the most common B-cell neoplasm, is characterized by overexpression of *bcl-2* through a t(14;18)(q32;q21) chromosomal translocation[25]. ABT-737 by itself was cytotoxic against the t(14;18) chromosomal translocation-containing lymphoma cell lines RS11380, DoHH2 and SuDHL-4 (median effective concentration $EC_{50} = 0.15 \pm 0.03\,\mu M$, $0.13 \pm 0.01\,\mu M$, and $0.85 \pm 0.14\,\mu M$, respectively; mean ± s.e.m., $n = 3$). The enantiomer was weaker by a factor of >29, suggesting that the activity was the direct result of binding to Bcl-X_L or Bcl-2. Moreover, ABT-737 significantly improved survival in a tumour model of disseminated disease using DoHH-2 cells (see Supplementary Fig. 4), confirming the activity observed in tissue culture.

To demonstrate that the cytotoxicity was not restricted to established tumour cell lines, we evaluated ABT-737 against primary patient-derived follicular lymphoma cells. ABT-737 (10–100 nM), but not the enantiomer, induced apoptosis in these samples (Fig. 3b). Similarly, ABT-737 induced concentration-dependent apoptosis in 13 of 15 patient-derived chronic lymphocytic leukaemia (CLL) B-cell specimens (Fig. 3c), while the enantiomer control had little effect at concentrations up to 100 nM.

Activity against SCLC-derived cells suggests that ABT-737 could also be useful for the treatment of solid tumours. The majority of SCLC cell lines studied were sensitive to ABT-737 ($EC_{50} < 1\,\mu M$),

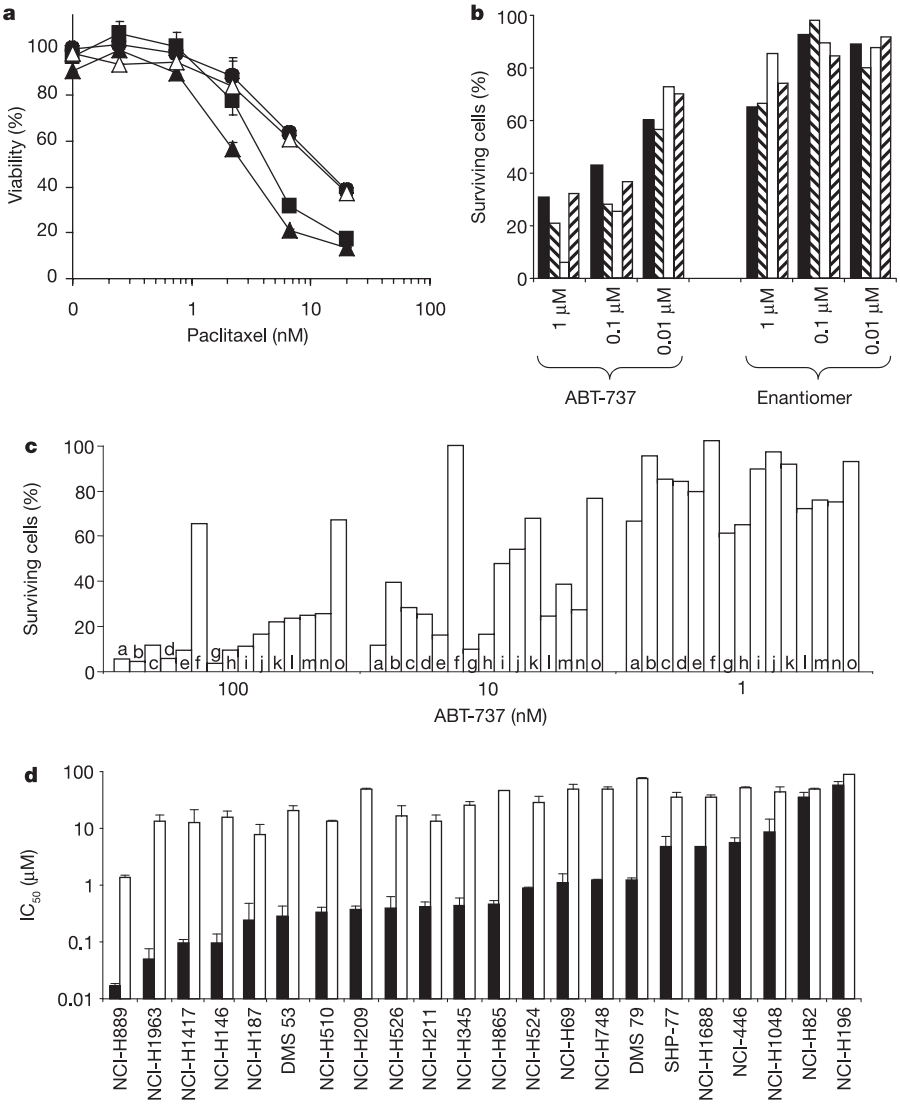

Figure 3 | Cell-based activity of ABT-737. **a**, ABT-737 enhances the activity of paclitaxel against A549 NSCLC cells. Filled circle, vehicle; filled square and filled triangle, 0.37 μM and 1.1 μM ABT-737, respectively; open triangle, 1.1 μM enantiomer. Data are mean ± s.d. **b**, **c**, ABT-737 induces apoptosis of primary follicular lymphoma cells (**b**) and primary CLL cells (**c**). Values are normalized to survival of untreated cells (bar pattern (**b**) and letters within bars (**c**) designate individual patient samples). CLL cell survival following enantiomer treatment is >76% and >87% at 100 nM and 10 nM, respectively. **d**, ABT-737 (filled bar), but not the enantiomer (open bar), is active against SCLC cell lines cultured in the presence of 10% human serum. Data are mean ± s.d.

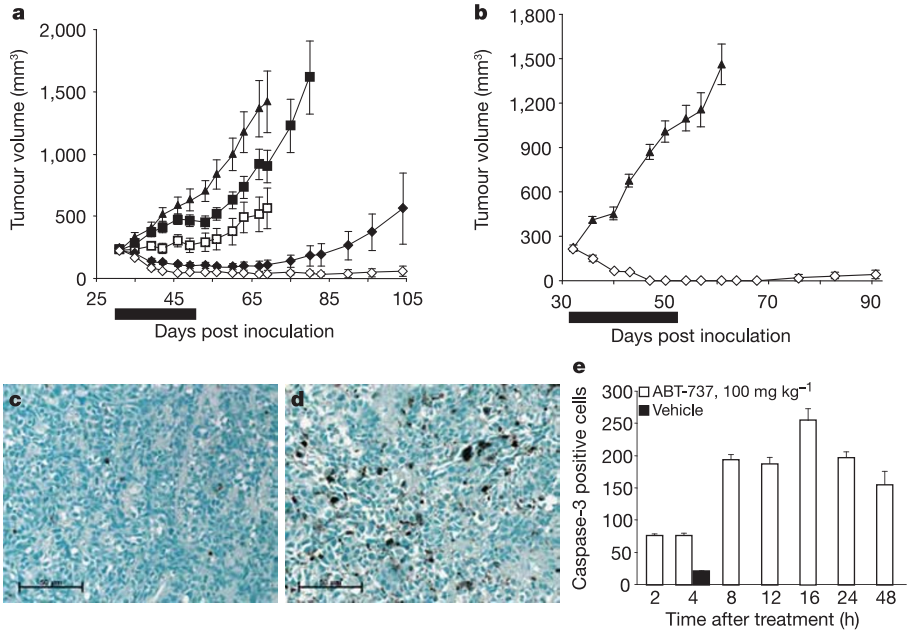

Figure 4 | *In vivo* anti-tumour activity of ABT-737. a, **b**, ABT-737 is efficacious in the H146 (**a**) and H1963 (**b**) SCLC xenograft models. Filled triangle, vehicle; filled square, ABT-737 administered i.p., 25 mg kg^{-1} day^{-1}; open square, 50 mg kg^{-1} day^{-1}; filled diamond, 75 mg kg^{-1} day^{-1}; open diamond, 100 mg kg^{-1} day^{-1} (complete regression of 77% H1963 tumours, and 77% and 20% of H146 tumours treated at 100 and 75 mg kg^{-1} day^{-1}, respectively. Regression was also observed in H889, H1417, H187, H128 and H345 xenograft models, data not shown). Black bar indicates dosing period, data are mean ± s.e.m. **c**–**e**, ABT-737 induces apoptosis *in vivo*. Caspase-3 staining of vehicle (<5% of total tumour cells, 4 h after administration) (**c**) or ABT-737 (100 mg kg^{-1}, 16 h after administration) (**d**) treated H146 tumours. **e**, Time course for induction of apoptosis. Data are mean ± s.e.m.

and the >30-fold reduced potency of the enantiomer supports Bcl-2/X_L-mediated activity (Fig. 3d). Furthermore, in the *in vivo* setting, ABT-737 caused complete regression of established SCLC tumour xenografts (Fig. 4a and b), and tumours did not grow back in a high percentage of the mice for the duration of the study (58 days or 107 days after the cessation of therapy for H146 and H1963 mouse models, respectively).

To demonstrate that tumour regression was the result of apoptotic cell death, established H146 tumours were treated with a single dose of ABT-737 and analysed with an antibody specific for activated caspase-3 (Fig. 4c–e). A significant increase in caspase-3-positive cells was noted as early as 2 h after treatment, with a 12-fold increase achieved within 16 h. Examination of liver, heart and intestine revealed no increase in caspase-3 activation in these normal tissues (data not shown). Furthermore, ABT-737 was well tolerated by all observable measures and did not produce significant weight loss (<5%) in mice treated for 21 days, although clinical pathology revealed a reduction in platelets and lymphocytes. Taken together, our results suggest that Bcl-2 family inhibitors may be useful for the treatment of lymphoma and SCLC as monotherapy and a wide variety of cancers when given in combination with chemotherapy or radiation.

METHODS

NMR-based screening and structural studies. Bcl-X_L, Bcl-2 and domain III of HSA were prepared as previously described[19,26,27]. NMR data were collected at 303 K on Bruker DRX500, DRX600 and DRX800 spectrometers. NMR-based screening was conducted as previously described[20]. Intermolecular and intra-protein distance restraints were obtained from three-dimensional ^{15}N- and ^{13}C-nuclear Overhauser effect spectroscopy (NOESY) data, and structure calculations were performed using a simulated annealing protocol using the program X-PLOR[28]. For the structure calculations, the protein was held fixed with the exception of those residues that form the ligand-binding site. NMR and structural statistics are given in Supplementary Tables 1–5.

Compound preparation and affinity. ABT-737 was synthesized as illustrated in Supplementary Fig. 1. K_i values were determined using competitive fluorescence polarization assays as described previously[29], and were calculated using the equation for the binding of two competing ligands to a protein[30] ($n = 3$, mean ± s.e.m.).

Cytochrome *c* release from isolated mitochondria. Mitochondria were isolated from the mouse cell line FL5.12, incubated with peptide or drug for 35 min in the presence or absence of activated Bid (caspase-8-cleaved Bid myristoylated in a reaction with myristoyl CoA and N-myristoyl transferease, Myr–Bid), and cytochrome *c* release was quantified as previously described[22].

Mammalian two hybrid assay. Full length Bcl-X_L and Bcl-X_S were cloned to the mammalian two hybrid system vectors pM DNA BD and pVP16 AD, respectively (BD Bioscience). Bcl-X_L (3 μg), Bcl-X_S (3 μg) and pG5CAT indicator plasmids (3 μg) were transfected into HeLa cells using Lipofectamine reagent (Invitrogen). After 24 h, cells were treated with compounds or DMSO for an additional 24 h. CAT activity was measured using CAT ELISA kit (Roche Applied Science). Inhibition was normalized to the DMSO control.

Confocal microscopy. Low-passage HeLa cells were transfected with Bcl-X_L and GFP-Bcl-G_S at a ratio of 10:1 using Lipofectamine plus reagent (Invitrogen). Time-lapsed imaging was performed using a laser-scanning confocal microscope MRC 1024-MP (BioRad) equipped with thermostage (Warner Instruments). The fluorescence of mitochondrial green fluorescent protein (GFP)–Bcl-G_S was excited with the 488-nm laser line and the Mitotracker red CMXRos (Molecular Probes) was excited with the 568-nm laser line. Confocal images were acquired 10 min after addition of the compound.

Cell culture of tumour cell lines. Cells were cultured with compound for 48 h in RPMI 1640 medium supplemented with 10% FBS, 1% sodium pyruvate, 4.5 g l^{-1} glucose, and 1% antibiotic-antimycotic. Viability was determined by MTS assay (Promega) For potentiation studies, A549 NSCLC cells were incubated with paclitaxel alone in serum-free medium for 24 h followed by ABT-737 or the enantiomer for 48 h ($n = 3$, mean ± s.e.m.).

Primary patient tumour samples. Follicular lymphoma cells from anonymized donors were grown on a feeder layer of CD40 ligand-expressing 3T3 cells in Iscoves Modified Dulbecco's Medium supplemented with 10% Human AB serum, penicillin 100 U ml^{-1}, streptomycin 100 μg ml^{-1}, 10 mM HEPES pH 7.4, and 2 mM L-glutamine for 40–44 h. For CLL specimens, peripheral blood was obtained from anonymized donors (samples a–g in Fig. 3c) or from patients who had given written informed consent (samples h–o in Fig. 3c). CLL cells were purified using Ficoll gradient and negative immunomagnetic selection, and were incubated in the same medium as the follicular lymphoma cells with the addition of transferrin (50 μg ml^{-1}) and insulin (5 μg ml^{-1}) for 48 h (samples a–g in Fig. 3c) or in RPMI 1640 medium, supplemented with 10%

FBS (fetal bovine serum) and penicillin/streptomycin and L-glutamine for 24 h (samples h–o in Fig. 3c). Cell death was quantified by fluorescence-activated cell sorting (FACS) analysis of annexin V-positive cells.

NCI-H146 and NCI-H1963 xenograft tumour studies. *Scid* (NCI-H146) or *scid-bg* (NCI-H1963) mice (Charles River Laboratories) were inoculated subcutaneously (s.c.) with 5×10^6 low-passage tumour cells mixed with Matrigel (BD Biosciences). Thirty-one days (NCI-H146) or thirty-two days (NCI-H1963) after inoculation, tumours were size-matched with an average volume of 225–230 mm^3 with therapy initiated the following day. ABT-737 is not orally bioavailable in mice and was given every day (q.d.) intraperitoneally (i.p.) for 21 days ($n = 9$–10 mice per group). Tumour volume was estimated by calliper measurements ($V = LxW^2/2$). Complete regression (cure) was defined as absence of measurable tumour at the end of the experiment. For i.p. administration, 1 g ml^{-1} stock solution of ABT-737 in DMSO was added to a mixture of 30% propylene glycol, 5% Tween 80, 65% D5W (5% dextrose in water), pH 4–5 (final concentration of DMSO $\leq$ 1%).

Immunohistochemistry. Mice with established H146 tumours were given a single i.p. injection of ABT-737 at 100 mg kg^{-1} and tumours were collected at various times for immunohistochemical staining for activated caspase-3 (rabbit anti-active caspase-3 at 1:400, BD Pharmingen). Caspase-positive cells were scored at 400 × magnification. The average number of positive cells per 0.0625 mm^2 area was determined from three separate fields in each of three independent tumour samples.

Received 10 December 2004; accepted 31 March 2005
Published online 15 May 2005.

1. Daniel, N. N. & Korsmeyer, S. J. Cell death: critical control points. *Cell* **116,** 205–219 (2004).
2. Kirkin, V., Joos, S. & Zörnis, M. The role of Bcl-2 family members in tumorigenesis. *Biochim. Biophys. Acta* **1644,** 229–249 (2004).
3. Amundson, S. A. *et al.* An informatics approach identifying markers of chemosensitivity in human cancer cell lines. *Cancer Res.* **60,** 6101–6110 (2000).
4. Reed, J. C. Promise and problems of Bcl-2 antisense therapy. *J. Natl Cancer Inst.* **89,** 988–990 (1997).
5. Letai, A., Sorcinelli, M. D., Beard, C. & Korsmeyer, S. J. Antiapoptotic Bcl-2 is required for maintenance of a model leukemia. *Cancer Cell* **6,** 241–249 (2004).
6. Klasa, R. J., Gillum, A. M., Klem, R. E. & Frankel, S. R. Oblimersen Bcl-2 antisense: facilitating apoptosis in anticancer treatment. *Antisense Nucleic Acid Drug Dev.* **12,** 193–213 (2002).
7. Kutzki, O. *et al.* Development of a potent Bcl-XL antagonist based on α-helix mimicry. *J. Am. Chem. Soc.* **124,** 11838–11839 (2002).
8. Tzung, S.-P. *et al.* Antimycin A mimics a cell-death-inducing Bcl-2 homology domain 3. *Nature Cell Biol.* **3,** 183–191 (2001).
9. Becattini, B. *et al.* Rational design and real time, in-cell detection of the proapoptotic activity of a novel compound targeting Bcl-X_L. *Chem. Biol.* **11,** 389–395 (2004).
10. Kitada, S. *et al.* Discovery, characterization, and structure—activity relationships studies of proapoptotic polyphenols targeting B-cell lymphocyte/leukemia-2 proteins. *J. Med. Chem.* **46,** 4259–4264 (2003).
11. Wang, J.-L. *et al.* Structure-based discovery of an organic compound that binds Bcl-2 protein and induces apoptosis of tumor cells. *Proc. Natl Acad. Sci. USA* **97,** 7124–7129 (2000).
12. Degterev, A. *et al.* Identification of small-molecule inhibitors of interaction between the BH3 domain and Bcl-X_L. *Nature Cell Biol.* **3,** 173–182 (2001).
13. Enyedy, I. J. *et al.* Discovery of small-molecule inhibitors of Bcl-2 through structure-based computer screening. *J. Med. Chem.* **44,** 4313–4324 (2001).
14. Walensky, L. D. *et al.* Activation of apoptosis *in vivo* by a hydrocarbon-stapled BH3 helix. *Science* **305,** 1466–1470 (2004).
15. Baell, J. B. & Huang, D. C. S. Prospects for targeting the Bcl-2 family of proteins to develop novel cytotoxic drugs. *Biochem. Pharm.* **64,** 851–863 (2002).
16. Petros, A. M., Olejniczak, E. T. & Fesik, S. W. Structural biology of the Bcl-2 family of proteins. *Biochim. Biophys. Acta* **1644,** 83–94 (2004).
17. Kelekar, A. & Thompson, C. B. Bcl-2-family proteins: the role of the BH3 domain in apoptosis. *Trends Cell Biol.* **8,** 324–330 (1998).
18. Huang, D. C. & Strasser, A. BH3-only proteins—essential initiators of apoptotic cell death. *Cell* **103,** 839–842 (2000).
19. Sattler, M. *et al.* Structure of Bcl-X_L-Bak peptide complex: Recognition between regulators of apoptosis. *Science* **275,** 983–986 (1997).
20. Shuker, S. B., Hajduk, P. J., Meadows, R. P. & Fesik, S. W. Discovering high-affinity ligands for proteins: SAR by NMR. *Science* **274,** 1531–1534 (1996).
21. Mao, H. *et al.* Rational design of diflunisal analogues with reduced affinity for human serum albumin. *J. Am. Chem. Soc.* **123,** 10429–10435 (2001).
22. Letai, A. *et al.* Distinct BH3 domains either sensitize or activate mitochondrial apoptosis, serving as prototype cancer therapeutics. *Cancer Cell* **2,** 183–192 (2002).
23. Wei, M. C. *et al.* Proapoptotic BAX and BAK: A requisite gateway to mitochondrial dysfunction and death. *Science* **292,** 727–730 (2001).
24. Fearon, E. R. *et al.* Karyoplasmic interaction selection strategy: A general strategy to detect protein-protein interactions in mammalian cells. *Proc. Natl Acad. Sci. USA* **89,** 7958–7962 (1992).
25. Tsujimoto, Y., Finger, L. R., Yunis, J., Nowell, P. C. & Croce, C. M. Cloning of the chromosome breakpoint of neoplastic B cells with the t(14;18) chromosome translocation. *Science* **226,** 1097–1099 (1984).
26. Petros, A. M. *et al.* Solution structure of the antiapoptotic protein bcl-2. *Proc. Natl Acad. Sci. USA* **98,** 3012–3017 (2001).
27. Mao, H., Gunasekera, A. H. & Fesik, S. W. Expression, refolding, and isotopic labeling of human serum albumin domains for NMR spectroscopy. *Protein Express. Purif.* **20,** 492–499 (2000).
28. Brunger, A. T. *X-PLOR Version 3.1* (Yale Univ. Press, New Haven/London, 1992).
29. Zhang, H., Nimmer, P., Rosenberg, S. H., Ng, S.-C. & Joseph, M. Development of a high-throughput fluorescence polarization assay for Bcl-X_L. *Anal. Biochem.* **307,** 70–75 (2002).
30. Wang, Z.-X. An exact mathematical expression for describing competitive binding of two different ligands to a protein molecule. *FEBS Lett.* **360,** 111–114 (1995).

Supplementary Information is linked to the online version of the paper at www.nature.com/nature.

Acknowledgements We thank T. J. Kipps, L. Rassenti, J. Gribben and L. Vallat for CLL Research Consortium samples, E. Monosov for assistance with confocal imaging, C. Rudin and C. Hann for H345 xenograft studies, and S. Ackler for compound formulation.

Author Information Atomic coordinates have been deposited in the Brookhaven Protein Data Bank under the accession codes 1YSG (Fig. 1a), 1YSI (Fig. 1b), 1YSX (Fig. 1c), 1YSN (Supplementary Fig. 2a), and 1YSW (Supplementary Fig. 2b). Reprints and permissions information is available at npg.nature.com/reprintsandpermissions. The authors declare competing financial interests: details accompany the paper on www.nature.com/nature. Correspondence and requests for materials should be addressed to S.H.R. (saul.rosenberg@abbott.com) or S.W.F. (stephen.fesik@abbott.com).